Uniform stochastic web in low-dimensional Hamiltonian systems

Sergey Pekarsky [1,2], Vered Rom-Kedar [*,3]

Department of Applied Mathematics and Computer Science, The Weizmann Institute of Science, Rehovot 76100, Israel

Abstract

When an unperturbed Hamiltonian is degenerate and some resonance conditions are satisfied a stochastic web is formed. A classical example of this phenomena is the wave–particle interaction in a constant uniform magnetic field. Recently, Dana has observed that for wide wave packets, the initial position of the cyclotron orbit center, x_c, may influence dramatically the diffusion of particles in phase space. A consistent method for finding the bare-web and the rigorous bounds on the separatrix splitting are derived for arbitrary position of the cyclotronic orbit center. The dramatic, sensitive dependence of the width of the stochastic layer on x_c is thus revealed. It is then argued that $x_c = 0$ corresponds to a nongeneric case, resolving contradictory results found for estimating the width of the stochastic layer in the commonly studied $x_c = 0$ case.

1. Introduction

In a general nondissipative physical system of sufficiently large dimension chaotic behavior is irremovable, meaning that under quite general conditions for most values of the parameters there exist some regions of phase space for which the system has chaotic dynamics. The number of degrees of freedom (d.o.f.) in the system N essentially determines whether these regions are isolated or form a connected web in the phase space. In case of a perturbation of a nondegenerate integrable system KAM theory [14] implies that for $N \leqslant 2$ invariant tori divide the phase space while for $N > 2$ some of the chaotic regions form a connected web which gives rise to Arnold's diffusion [3]. The minimal dimensionality of a system in which chaotic regions appear is $N_{min} = 1\frac{1}{2}$ corresponding to a time-dependent perturbation of an autonomous d.o.f. Hamiltonian system.

It follows that near integrable nondegenerate 1.5 d.o.f. Hamiltonian systems are stable near elliptic fixed points; under sufficiently small perturbations KAM tori bound a finite size neighborhood from escaping [4] (though in the resonant case local instabilities may occur). Surprisingly, Zaslavsky et al. [28] have found that *degenerate* near-integrable 1.5 d.o.f. Hamiltonian systems may become globally unstable for infinitesimal

---

* Corresponding author.
[1] Current address: Department of Control and Dynamical Systems, Caltech, Pasadena, CA 91125, USA.
[2] E-mail: pekarsky@wisdom.weizmann.ac.il.
[3] E-mail: vered@wisdom.weizmann.ac.il.

resonant perturbation. A stochastic web is then observed in the phase space – there exists a web of split separatrices leading to nearby chaotic motion which is unbounded in space. The width of the chaotic region along the web may be approximately constant in the whole space (a uniform web) or exponentially diminishing with the distance – making the web effectively finite. A fundamental example for this phenomena is the wave-particle interaction in a constant uniform magnetic field; a uniform web is created by an *infinitely wide* electrostatic wave packet whereas a single harmonic wave produces an exponentially diminishing web (see Ref. [25]). Variations on this example appear in numerous applications in plasma physics [16,25].

While uniform stochastic webs are nongeneric and are probably structurally unstable, nearby systems are vastly influenced by the web's global instabilities. This exemplifies the general notion that singular, nongeneric systems are worth studying not only because of their mathematical beauty, but also because of their strong impact on neighboring systems. Indeed, though in the plasma physics applications the conditions for generating a uniform stochastic web (degeneracy, resonance, infinitely wide wave packet) may be only approximately fulfilled, the underlying instabilities of the web are clearly felt [28].

The general Hamiltonian describing a periodically kicked charge in a uniform magnetic field has the form

$$H = \frac{\mathbf{P}^2}{2m} + K_0 V(kx) \sum_{n=-\infty}^{\infty} \delta(t - nT), \tag{1}$$

where $\mathbf{P} = \mathbf{p} - (q/c)\mathbf{A}$ is the kinetic momentum of a particle with charge q and mass m in a uniform magnetic field $\mathbf{B}$ (in the z-direction, with vector potential $\mathbf{A}$), K_0 is a parameter, k is the wave-vector taken in the x-direction, V is a general periodic potential with period 2π, and T is the period. Introducing dimensionless variables $u = P_x/\omega_0$ and $v = P_y/\omega_0$ ($\omega_0 = qB/c$ is the cyclotron frequency), setting, with no loss of generality $m = k = 1$, and using $x_c = x + P_y/\omega_0 = x + v$, (1) becomes [30,7],

$$H = \omega_0 \frac{u^2 + v^2}{2} + K_0 V(x_c - v) \sum_{n=-\infty}^{\infty} \delta(t - nT). \tag{2}$$

with the canonical conjugate pairs (u, v) and (x_c, y_c), the latter being the coordinates of the center of a cyclotron orbit. As long as H is independent of y_c, the cyclotron x coordinate, x_c, is a constant of motion.

Analysis of this model was mainly done under the tacit assumption $V(x) = -\cos(x)$, $x_c = 0$ (e.g., see Ref. [30]). Then, in the resonance case $\alpha \equiv \omega_0 T = 2\pi m/n$, a stochastic web appears for arbitrarily small values of K_0. In the singular small K_0 limit there exists a "bare web" corresponding to an integrable Hamiltonian with infinite web of heteroclinic connections, which is singularly perturbed by an infinite tail of harmonics.

Some nonrigorous methods have been applied to obtain the bare web structure and the effect of the tail of harmonics. For $x_c = 0$, this leads to qualitative correct results, i.e. the structure of the bare web was discovered and exponentially small (in K_0) splitting distances were predicted [1,17]. However, it appears that different nonrigorous schemes produce different results, even for the exponential factor of the splitting distance, see Appendix A. Moreover, a simple application of these schemes to an odd potential ($x_c = \pi/2$) produces no information regarding the bare web (Dana, private communication).

Dana [7], and Dana and Amit [6] have shown numerically that the structure of the web and the diffusion along it vary considerably as x_c is varied. Here, we set forth the theoretical foundations for the analysis of the bare web and the separatrix splitting for general x_c in the limit of small K_0. Physically, a general ensemble of particles is expected to have a distribution of x_c values [6]. Moreover, any y_c dependence of V will cause x_c to vary – thus a study of the $x_c = \text{const} \neq 0$ is bound to appear in some averaged framework. Finally, if the electric field is nontransverse to the magnetic field [29], the longitudinal coordinate plays a similar role to x_c, see Ref. [21]. Beyond the physical reasons for studying the general x_c case, we show that these considerations produce an explanation to the contradictory nonrigorous results found for $x_c = 0$.

As in Ref. [30], consider the Poincaré map that corresponds to the general Hamiltonian with arbitrary value of x_c and choose the potential to be of the standard type, $V(x) = -\cos(x)$. Then the following mapping with a twist is obtained [6],

$$M_\alpha : \quad \bar{u} = [u + K\sin(v - x_c)]\cos\alpha_q + v\sin(\alpha_q),$$

$$\bar{v} = -[u + K\sin(v - x_c)]\sin\alpha_q + v\cos(\alpha_q), \tag{3}$$

where $K = K_0/T$ and the primary resonance condition $\alpha_q \equiv \omega_0 T = 2\pi/q$ is satisfied for some integer q. Henceforth the case $q = 4$ (the "web-map"), which is one of the crystalline-type symmetric webs, will be analyzed

$$M_4 : \quad u' = v, \qquad v' = -u - K\sin(v - x_c). \tag{4}$$

This mapping is obviously simplectic and, loosely speaking, corresponds to a kick followed by a rotation by $\pi/2$. A central observation is that the fourth iterate of the web-map M_4^4 is an analytical near identity mapping [30,18]; Hence, a whole machinery developed for the analysis of near identity diffeomorphisms (see, e.g., Refs. [9,10,2]) can be applied. Using this machinery we find rigorous results regarding the bare-web structure and the sequence of bifurcations it undergoes as x_c is varied. Moreover, rigorous upper bounds on the separatrix splittings are found.

The paper is organized as follows. In Section 2 the bare web is constructed, and its bifurcations as x_c is varied are found. In Section 3 estimates for the separatrix splitting and the width of the stochastic layer are derived. These estimates are compared with numerical results in Section 4; the issue of the transport in the system is also addressed there. In the last section we discuss possible applications of these results.

2. Uniform web structure

In the first part of this section the symmetries of the map (4) are found. In the second part the asymptotic behavior for small K is investigated.

For general, fixed, x_c, the map possesses the following time reversal symmetry,

$$M_4^{-1} = S \circ M_4 \circ S, \tag{5}$$

where $S : \{u' = v, \ v' = u\}$ is a reflection with respect to the $u = v$ line. For particular values of x_c additional symmetries arise; for $x_c = 0$ or π there is an exact Z_2 symmetry: $u \to -u$, $v \to -v$. For $x_c = \pi/2$ the map is invariant under the following transformations: $u \to -u + \pi$, $v \to -v + \pi$.

The map is also invariant, up to a shift, with respect to simultaneous translations or inversions of coordinates and the constant x_c. The transformations

$$x_c \to x_c + \pi, \qquad v \to v + \pi, \qquad u \to u + \pi$$

$$x_c \to -x_c, \qquad v \to -v, \qquad u \to -u, \tag{6}$$

introduce a 2π shift or no shift in v, respectively. Thus, x_c may be restricted to range from 0 to $\pi/2$.

To analyze the properties of this map for small K consider its fourth iterate,

$$\bar{u} = u + K\sin(v - x_c) + K\sin\{v + x_c - K\sin[u + K\sin(v - x_c) + x_c]\},$$

$$\bar{v} = v - K\sin(\bar{u} - x_c) - K\sin[u + K\sin(v - x_c) + x_c], \tag{7}$$

which produces a near identity mapping. The limit $K \to 0$ of this map corresponds to a singular perturbation of a system of differential equations, which is found by replacing the difference operator $\bar{u} - u$ of (7) with

a differential [9,2], and expanding the right hand side in K. The system thus obtained corresponds to the Hamiltonian flow of

$$H = -(K/2)(\cos u + \cos v)\cos x_{\rm c} - (K^2/4)\sin(u + x_{\rm c})\sin(v + x_{\rm c}) + O(K^3). \tag{8}$$

The level set $H = 0$ of the Hamiltonian (8) describes the approximate structure of the bare web. Other level sets describe the "web-tori" which are nested in the web cells. Refs. [30,17] have used this approach and another heuristic "averaging" approach to obtain the bare web for the case $x_{\rm c} = 0$. The two approaches give the same results to linear order in K, while the "averaging" method does not produce nonlinear terms in K. Since for $x_{\rm c} = \pi/2$ the first order terms in K vanish, the analysis near $x_{\rm c} = \pi/2$ must include higher order terms.

Thus, to proceed, we divide the $x_{\rm c}$ range into two main regions:
– The *diamond lattice* region: $x_{\rm c} \in [0, \pi/2] \setminus I_\alpha$.
– The *square lattice* region: $x_{\rm c} \in I_\alpha = [\pi/2 - \alpha K, \pi/2], \alpha = O(1)$.
Recall that by symmetry (6) it is sufficient to consider only these regions.

Consider the diamond lattice first. Fixed points of the Hamiltonian equations (equivalently of M_4^4) can be found perturbationally in K,

$$u_0 = \pi m + (-1)^{|n|}(K/2)\sin x_{\rm c}, \qquad v_0 = \pi n + (-1)^{|m|}(K/2)\sin x_{\rm c}. \tag{9}$$

Linearization in the neighborhood of these fixed points shows that they are elliptic for $m + n = 2l$ and hyperbolic for $m + n = 2l + 1$, with eigen-values proportional to $K\cos(x_{\rm c})$. In the later case heteroclinic connections of stable and unstable manifolds form a connected web. For $K \to 0$ they correspond to the lines $v = \pm u + (2j+1)\pi$, producing the diamond lattice (Fig. 1a).

Now, consider the square lattice, for which $x_{\rm c} \in I_\alpha$ i.e. $x_{\rm c} = \pi/2 - \rho K$ and ρ is of order 1. It turns out that at least third order terms in K of the Hamiltonian (8) are needed to unfold the bifurcations of the bare web in this regime of $x_{\rm c}$. Expanding the right hand side of (7) to third order in K we find

$$H = -(K/2)(\cos u + \cos v)\cos x_{\rm c} - (K^2/4)\sin(u + x_{\rm c})\sin(v + x_{\rm c})$$
$$+ (K^3/8)[\cos(v + x_{\rm c})\sin^2(u + x_{\rm c}) + \cos(u + x_{\rm c})\sin^2(v + x_{\rm c})]. \tag{10}$$

Thus, perturbationally in K, there are three families of fixed points of the corresponding Hamiltonian equations.
(i) Fixed points defined by the conditions

$$\sin u = \sin v = K/2, \tag{11}$$

which are elliptic centers for any value of ρ except for the region

$$\tfrac{1}{2} < |\rho| < \rho_-, \qquad \rho_- = \frac{1}{2}\frac{1 + 3K^2/2}{1 + K^2}, \tag{12}$$

where half of them become hyperbolic. Namely, for $\rho > 0$ fixed points determined by the condition $\cos u, \cos v > 0$ become hyperbolic while the rest are elliptic, and for $\rho < 0$ fixed points determined by the condition $\cos u, \cos v < 0$ become hyperbolic while the rest are elliptic. The bifurcating points are the centers from which fixed points (15) are born.
(ii) Fixed points defined by the conditions

$$\sin u = \sin v = -K/2, \tag{13}$$

which are hyperbolic, with eigenvalues proportional to K^2, for $|\rho| > \rho_+$ and elliptic for $|\rho| < \rho_+$, where

$$\rho_+ = \tfrac{1}{2}\sqrt{1 - 3K^2/2}, \qquad \rho_+ < \tfrac{1}{2}. \tag{14}$$
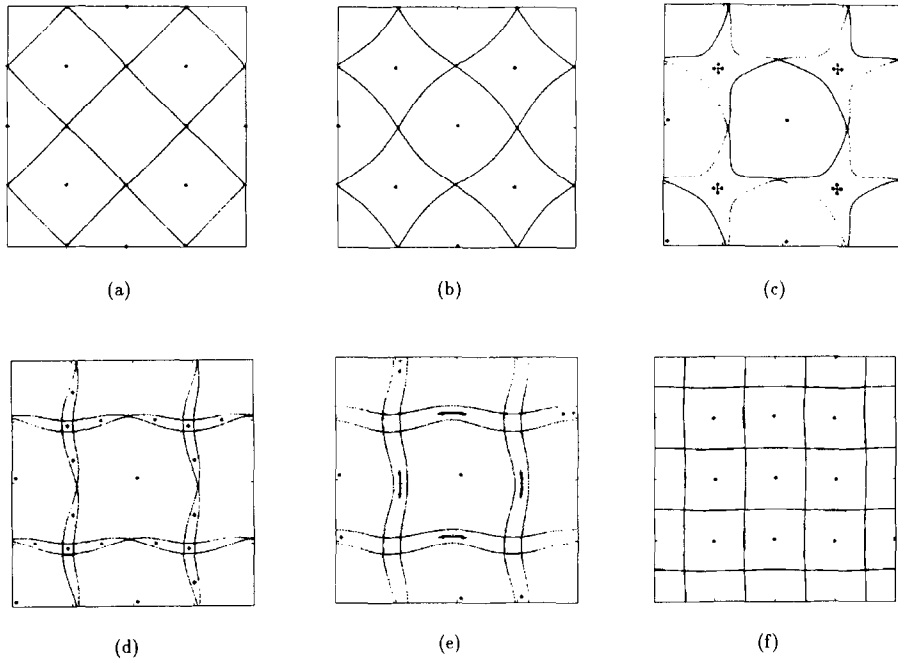
Fig. 1. Structure of the stochastic web for different values of parameters. (a) $K = 0.1, x_c = 0$; (b) $K = 0.1, x_c = 1.45$; (c) $K = 0.5, x_c = 1.3208$; (d) $K = 0.5, x_c = 1.3307$; (e) $K = 0.5, x_c = 1.3451$; (f) $K = 0.1, x_c = 1.5708$.

(iii) Fixed points defined by the conditions

$$\cos u = \cos v = \rho(2 - \sqrt{1 - 4\rho^2 K}),\tag{15}$$

which are hyperbolic, with eigenvalues proportional to K^2, and exist only for $0 \leqslant |\rho| < \frac{1}{2}$.

For $x_c = \pi/2$ ($\rho = 0$) the bare web consists of heteroclinic connections between the hyperbolic fixed points of (15) which connect in a square lattice (Fig. 1f). It follows that a global bifurcation must occur for $\rho_+ < \rho < \frac{1}{2}$ (see Fig. 1c and 1e).

Fig. 1 shows the numerical realization of a sequence of bifurcations that occur in the web-map for small K ($K = 0.1, 0.5$), when x_c changes from 0 to $\pi/2$. It is seen that the analysis supplies accurate predictions for the changes in the phase portrait. However, we note that while the corresponding level sets of (10) coincide with the bare web of the map for $x_c \notin I_\alpha$, for $x_c \in I_\alpha$ there are differences even in the asymptotic limit.

For $x_c = 0$ the phase portrait is well-known and represents a symmetric infinite web inside each cell of which there are cross sections of invariant tori (Fig. 1a). All cells are identical and of the area $2\pi^2$. When x_c is increased [4] the separatrices undergo deformation; at the same time, elliptic and hyperbolic fixed points shift in opposite directions (9) breaking Z_2 symmetry (Fig. 1b). At $x_c = \pi/2 - \rho_- K$, where ρ_- is defined by (12), half of the elliptic centers (11) become hyperbolic, with the *sign* of ρ determining the position of the bifurcating points [5]. Then, at $x_c = \pi/2 - K/2$ these fixed points change their stability back, and, at the same time, four hyperbolic fixed points (15) are born from them (Fig. 1c and Fig. 2). Heteroclinic intersections corresponding to these saddles form a new web that merges with the old one at the global bifurcation (Fig. 1d). Then at $x_c = \pi/2 - \rho_+ K$, where ρ_+ is defined by (14) another local bifurcation occurs (Fig. 1e) and (13) becomes stable. Finally, for $x_c = \pi/2$ a new symmetric infinite web with cells of the area π^2 is formed,

---

[4] In fact, similar phenomena occur when K is increased, thus, K was taken 0.1 in Figs. 1a, 1b, 1f.

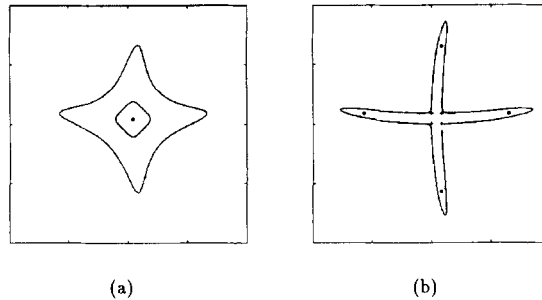[5] This bifurcation was not detected numerically.

Fig. 2. Enlargement of the local bifurcation of Fig. 1c; the size of the square is 1.9×1.9; $K = 0.5$; (a) $x_c = 1.32$; (b) $x_c = 1.321$.

(Fig. 1f), these cells being half the size the diamond lattice cells. Further increase in x_c causes the above sequence of bifurcations to repeat itself in the reverse order and with the position of the bifurcating centers (11) interchanged. When the value of $x_c = \pi$ is reached the phase portrait is identical to the case $x_c = 0$.

3. Stochastic layer

The bare webs found in Section 2 consist of coinciding stable and unstable manifolds of hyperbolic fixed points. It is well known that under small perturbations, i.e. for any finite K, these manifolds generically split. The splitting distance, in this singular setting, is expected to be exponentially small. Rigorous upper bounds[6] on the exponential factor of the splitting distance are easily obtained in Section 3.1 by applying Fontich and Simó's [9] results for the square and diamond lattices. More elaborate schemes may be used to estimate the power-law [15,10,2] and even the constant factors of the splitting distance [26], however this is beyond the scope of this paper. In Section 3.2 the heuristic approach of [1] is adapted to find nonautonomous perturbation for the bare web. Formal estimates of the separatrix splitting are then found using the usual Melnikov technique [20]. $x_c = 0$ is found to be a nongeneric perturbation for which the leading order exponential factor has a zero coefficient.

Gelfreich et al. [10] proved that the width of the instability zone created by the separatrix splittings is proportional to the angle of the separatrix splitting. Determining more precisely the thickness of the chaotic region is hindered theoretically and computationally, as in the usual near-integrable 1.5 d.o.f. systems, by the appearance of islands, of sticky islands, and the abrupt breaking of the web-tori. Approximating the orbits near the web by the separatrix mapping leads to estimates of this thickness [27,30,5]. Measuring it numerically confirms at least the exponential factor dependence which is found by the heuristic calculations.

3.1. Separatrix splittings in the web-map

Fontich and Simó [9] considered analytic near identity diffeomorphisms with limiting flows attaining heteroclinic or homoclinic connections. Using the Birkhoff normal form, they have established exponentially small upper bounds on the splittings of the separatrices for small perturbation parameter K. The exponent is related to the complex singularities of the homoclinic/heteroclinic solutions of the limiting flow

$$\Delta h \approx N \exp(-2\pi\delta/\ln \Lambda), \tag{16}$$

---

[6] Lower bounds for the separatrix splittings in the near-identity limit have been established only for the extensively studied standard map by using a computer-assisted proof [15].

where $|\ln(N(K))| \ll |-2\pi\delta/\ln\Lambda|$ as $K \to 0$, δ is the distance from the real axis to the nearest singularity of the homoclinic orbit of the unperturbed flow, and Λ is the larger eigenvalue of the linearized diffeomorphism near the hyperbolic fixed point.

Since M_4^4 is an analytic near identity map which may be put in the form considered in Ref. [9], (16) is applicable for the estimation of the upper bound on the splitting distance Δh:

- For the diamond lattice case ($x_c \notin I_\alpha$), the limiting Hamiltonian flow

$$H = -(K/2)\cos x_c(\cos u + \cos v) = -\Omega(\cos u + \cos v), \tag{17}$$

has hyperbolic fixed points (9). Its heteroclinic solutions are

$$\sin u = -\sin v = -\frac{1}{\cosh \Omega t} = -\frac{1}{\cosh \tau}, \tag{18}$$

where $\Omega = \frac{1}{2}K\cos x_c$ (recall that the deformation seen in Fig. 1 for $x_c \neq 0$ comes from $O(K^2)$ terms) and τ is the appropriate rescaled time of the Hamiltonian flow. Their closest singularities to the real axis are at $\tau = \pm i\pi/2$, hence $\delta = \pi/2$. The larger eigenvalue of the linearized diffeomorphism is equal to $\Lambda = 1 + 2K\cos x_c$, and $\ln \Lambda = 2K\cos x_c$ Thus

$$\Delta h = N\exp\left(-\frac{\pi^2}{2K\cos x_c}\right). \tag{19}$$

- For the square lattice ($x_c \in I_\alpha$), the limiting Hamiltonian flow

$$H = \frac{\rho K^2}{2}(\cos u + \cos v) - (K^2/4)\cos u \cos v \tag{20}$$

has hyperbolic fixed points (15). Separatrices for small deviations from $\pi/2$ do not differ substantially from those at $x_c = \pi/2$, which are given by horizontal and vertical lines,

$$u = \pm\frac{1}{\pi/2}, \qquad \cos v = \mp\frac{1}{\cosh K^2 t/4} = \mp\frac{1}{\cosh \nu} \tag{21}$$

and

$$v = \pm\frac{1}{\pi/2}, \qquad \cos u = \mp\frac{1}{\cosh K^2 t/4} = \mp\frac{1}{\cosh \nu}, \tag{22}$$

where $\nu = \frac{1}{4}K^2 t$ is the rescaled time. The closest singularities to the real axis is at $\tau = \pm i\pi/2$, hence, again, $\delta = \pi/2$. The larger eigenvalue of the linearized diffeomorphism is equal to $\Lambda = 1 + K^2$, and $\ln \Lambda = K^2$. Thus

$$\Delta h = N\exp(-\pi^2/K^2). \tag{23}$$

Here N is some function of K and x_c.

(19) and (23) provide rigorous upper bounds on separatrix splittings in the web-map. In the next section perturbation of the integrable Hamiltonian flow will be considered and nonrigorous estimates for the thickness of the stochastic layer will be derived.

3.2. Perturbation of the web-flow

Consider the following perturbation of the bare web Hamiltonian [29],

$$V = -K \cos x_c \sum_{m=1}^{\infty} [\cos v + (-1)^m \cos u] \cos \pi m t$$

$$- K \sin x_c \sum_{m=1}^{\infty} [\sin v \cos \pi(m - 1/2)t + (-1)^m \sin u \sin \pi(m - 1/2)t]. \tag{24}$$

It was obtained by reordering the infinite sum of the δ functions in tuples of 4, corresponding heuristically to some averaging procedures. This procedure produces naturally only linear terms in K. Further only the first harmonic in (24) will be retained. Thus, V corresponds to a time-periodic perturbation of the Hamiltonians (17) and (20), and the splitting distance between the manifolds may be formally calculated by using the Melnikov integral – the integral of $\{H, V\}$ along the unperturbed separatrices. Then, one may use these results to estimate the width of the stochastic layer by constructing the separatrix mapping

$$H_{n+1} = H_n + M(t_n), \qquad t_{n+1} = t_n + \tfrac{1}{4} P(H_{n+1}).$$

Here $P(H)$ denotes the period function of orbits inside the cell and $M(t)$ is the Melnikov function,

$$M(t_0) = \int_{-\infty}^{\infty} \{H(q^0(t)), V(q^0(t), t + t_0)\} \, dt = M_1(t_0) + M_2(t_0), \tag{25}$$

where M_1, M_2 correspond to different harmonics of the perturbation (24), and the integration is along the solutions (18) or (21).

Consider separately the two regions of possible values of x_c:

(i) For the diamond shape lattice, $x_c \notin I_\alpha$, straightforward calculations of (25) along (18) give, after substituting exp for cosh and sinh

$$M(t_0) = -8\pi^2 \cos \pi t_0 \exp(-\pi^2/2\Omega) - 2\pi^2 \tan x_c \left(\sin \frac{\pi t_0}{2} - \cos \frac{\pi t_0}{2} \right) \exp(-\pi^2/4\Omega), \tag{26}$$

Then, the separatrix mapping is given by the following expression,

$$H_{n+1} = H_n - 8\pi^2 \cos \pi t_n \exp(-\pi^2/2\Omega) - 2\pi^2 \tan x_c \left(\sin \frac{\pi t_n}{2} - \cos \frac{\pi t_n}{2} \right) \exp(-\pi^2/4\Omega),$$

$$t_{n+1} = t_n + \frac{1}{\Omega} \ln \left(\frac{8\Omega}{|H_{n+1}|} \right),$$

where asymptotics near the separatrix for the period T have been used. The width of the stochastic web is estimated using the following condition [30],

$$\max \left\| \frac{\delta t_{n+1}}{\delta t_n} - 1 \right\| > 1,$$

which is a rough criterion of local instability present in the phase space. Hence, the border of stochasticity region is defined by

$$H_s = \frac{2\pi^3}{K \cos x_c} [\tan x_c \exp(-\pi^2/2K \cos x_c) + 8 \exp(-\pi^2/K \cos x_c)]. \tag{27}$$

Note that for general x_c and for small K the second term is much smaller than the first one. However, the first term vanishes for $x_c = 0$. Thus, $x_c = 0$ corresponds to a nongeneric case (see Appendix A).

(ii) Consider the square lattice case, i.e. $x_c = \pi/2 + \rho K$ and $|\rho| \leqslant 1$. The Melnikov function is given by

$$M(t_0) = \int_{-\infty}^{\infty} \dot{H}(t, t_0) \, dt = \frac{K^3}{4} \int_{-\infty}^{\infty} \cos v(\cos v - 2\rho) \cos(\pi(t + t_0)/2) \, dt,$$

where integration is performed along separatrix (21). Upon integration and substituting exp for cosh and sinh

$$M(t_0) = 2\pi K \cos \frac{\pi t_0}{2} \left(\frac{\pi}{K^2} - \rho \right) \exp(-\pi^2/K^2). \tag{28}$$

Thus, the separatrix mapping has the following form,

$$H_{n+1} = H_n + \frac{2\pi^2}{K} \cos \frac{\pi t_n}{2} \exp(-\pi^2/K^2), \qquad t_{n+1} = t_n + \frac{4}{K^2} \ln \frac{K^2}{|H_{n+1}|},$$

where the period of the motion near the separatrix $T(H) = (16/K^2) \ln(K^2/|H|)$ was used (see Ref. [30]) and we have neglected ρ comparing to π/K^2.

Finally, the border of stochastic layer is determined by

$$H_s = \frac{4\pi^3}{K^3} \exp(-\pi^2/K^2). \tag{29}$$

Note that the expression in the exponent is proportional to $1/K^2$ and not to $1/K$ as it is in (27). This implies that the stochastic layer is much smaller when x_c belongs to the neighborhood of $\pi/2$ or $3\pi/2$.

Notice the general agreement between formulas (19) and (26), and (23) and (28), respectively. The difference is only in the case $x_c = 0, \pi$ when the leading term in (27) vanishes due to $\tan x_c$ being equal to 0. But, as mentioned above, this corresponds to a nongeneric case, and the general upper bounds (16) cannot capture it. Hence, we can conclude that Hamiltonian (8) and its perturbation in the form (24) give correct asymptotic results to exponential order for the width of stochastic layer for the whole range of x_c, except possibly tiny intervals near $x_c = \frac{1}{2}(\pi \pm K)$ that correspond to a cascade of bifurcations, and thus are extraordinarily difficult to describe analytically.

4. Numerics – stochastic layer width and transport

Obtaining numerical estimations for asymptotically small K requires introduction of sophisticated arithmetics [9] or numerical schemes in the complex plane [15,2] in order to avoid errors induced by machine precision. Since only exponential factors are sought here, we avoid these problems by keeping the range of K values above 0.4. Furthermore, here the width of the stochastic layer is sought; locating its precise boundary, determined by the last KAM torus, is hindered by the complicated fractal structure of the stochastic layer.

Nevertheless, one can see from Fig. 3 that agreement between analytical and numerical results is very good. Dependence of the web's width on the value of the parameter x_c for fixed K is shown in Fig. 4. One sees that $x_c = 0$ corresponds, as predicted by (27), to a nongeneric case.

To examine the influence of the changes in the separatrix splittings on the transport of particles in phase space, numerical simulations of many-particles (10^3) evolution are performed. The diffusion coefficient, defined as the average of the particle distances square divided by the number of iterates,

$$D = \frac{\langle u^2 + v^2 \rangle}{N},$$

is measured as a function of K and x_c. Three factors which vastly influence such a computation are the numerical errors introduced by the computation, the choice of the initial ensemble of the particles and the
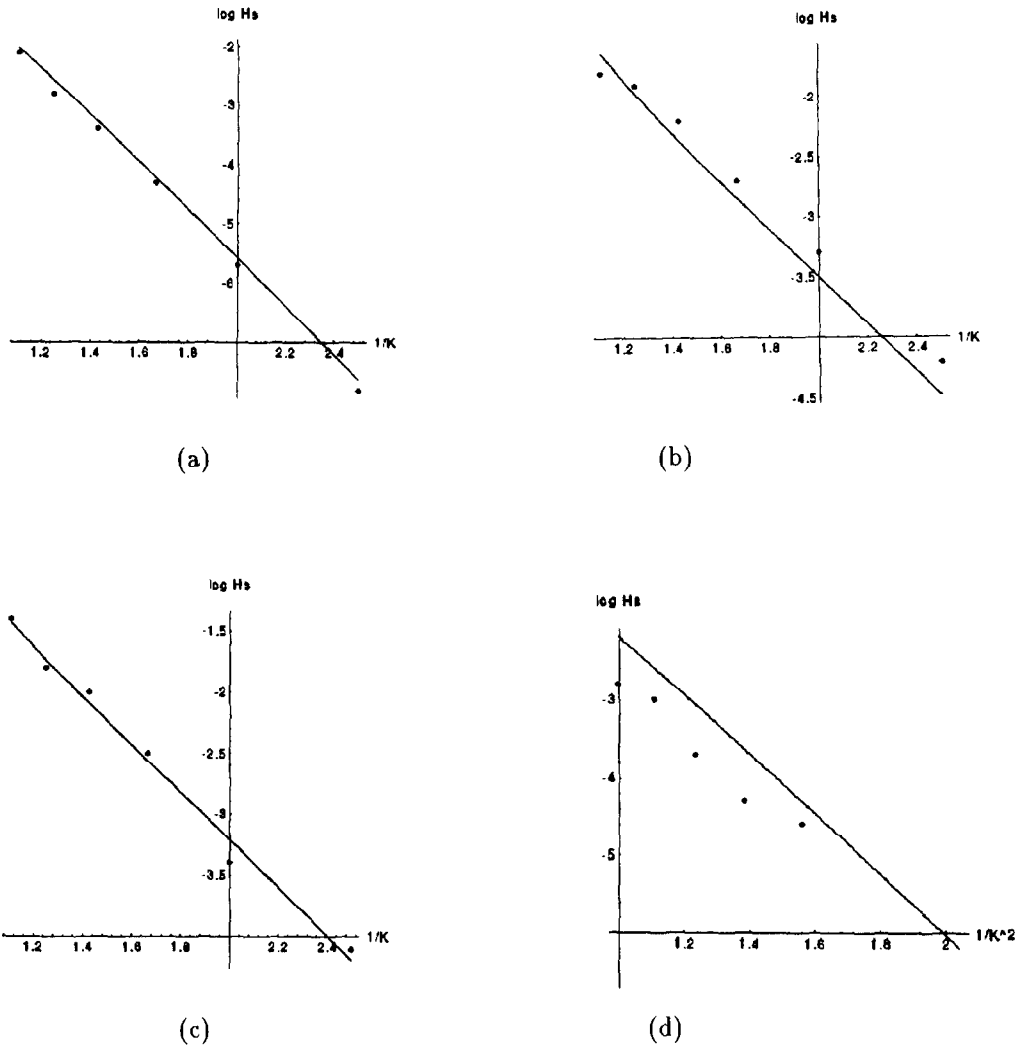
(a)

(b)

(c)

(d)

Fig. 3. Logarithmic width of the web. Comparison of analytical estimates (27) and (29) (continuous line) and numerical results (points) for various parameter values; (a) $x_c = 0$; (b) $x_c = 0.05$; (c) $x_c = 0.1$; (d) $x_c = \pi/2$.

simulation time N. Lattice maps (see Ref. [8] and references therein) and shadowing theorems [22,13,12] may be used to establish that long-term numerical computations of chaotic trajectories represent true orbits of a Hamiltonian system. In practice, no essential differences between floating point and lattice-map simulations were observed for $N = 10^4$. On the other hand the value of N and the method of selecting the initial ensemble vastly influence the results.

Below we summarize the results for the diffusion character and coefficients obtained by using the same type of initial ensembles and sufficiently large N ($N = 10^5 > 300\times$ turn-over time):

(i) Diffusion is uniform in all directions. Introduce coordinates $R^2 = u^2 + v^2$, $\phi = \tan(u/v)$. Then, for any values of parameters K and x_c the distribution of the angle ϕ on $[-\pi/2, \pi/2]$ has mean approximately 0 and variation approximately $\pi^2/12 \approx 0.8$, as the deviation of a uniform distribution on $[-\pi/2, \pi/2]$.

(ii) Diffusion for $x_c = 0$ is substantially smaller than for small positive values of x_c; for $K < 1$ the diffusion coefficient at $x_c = 0$ is approximately half of the diffusion coefficient at $x_c = 0.1$. This fact again indicates that
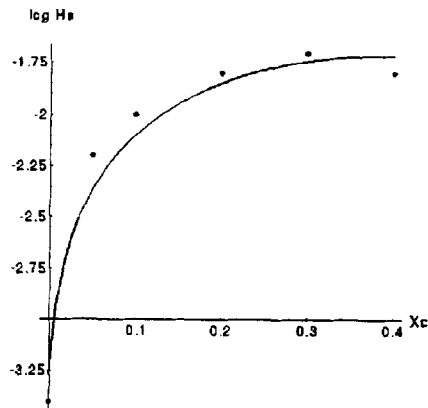
Fig. 4. Dependence of the web's width on the value of the parameter x_c for fixed $K = 0.7$.

$x_c = 0$ is a nongeneric value, and is in agreement with results for the width of stochastic layer (see (27) and Figs. 4 and 3).

(iii) Diffusion is extremely weak for $x_c \approx \pi/2$; the diffusion coefficient for $K < 1$ at $x_c = \pi/2$ is by order of magnitude smaller than the diffusion coefficient at $x_c = 0.1$. This shows the physical realization of the change in the character of the web near $x_c = \pi/2$.

The above results are obtained using the standard choice for the ensemble – namely picking up the initial conditions randomly in a close vicinity of a hyperbolic saddle and then excluding regular trajectories from the averaging. An alternative approach would be choosing initial points in a lobe, the area between consecutive intersections of the stable and unstable manifolds. There are two advantages to this approach; first, all information may be gathered by considering lobe intersections [23,24], hence, no questions regarding the validity of the ensemble arise. Second, by choosing initial conditions in the lobe it is guaranteed that no initial conditions belong to stable islands of one cell. (Though they may belong to elliptic islands visiting several cells, like the accelerating modes. These are expected to be small for small K.)

5. Conclusions and discussions

The bare stochastic web formed in the phase space changes its patterns as the coordinate of the cyclotron orbit center x_c is changing. This transition is accompanied by a series of local bifurcations associated with the change of stability of fixed points. Moreover, a global saddle connection bifurcation occurs symbolizing transition between diamond and square web structures. The hyperbolic saddles change their stability as x_c is varied. This fact has important consequences for the analysis of the full $2\frac{1}{2}$ d.o.f. system, which is produced when the potential V in (2) depends on y_c or when longitudinal degree of freedom is added due to oblique propagation of the wave packet.

Rigorous upper bounds on the splitting distance reveal a sensitive dependence on the value of x_c, with a different exponential dependence for general x_c and for x_c near $\pi/2$; the exponential proportional to $1/K$ and $1/K^2$ for the diamond and square lattices, respectively. Moreover, (27) and Fig. 4 suggest that $x_c = 0$ corresponds to a nongeneric case, for which the coefficient of the leading order term of the splitting distance vanishes. This fact leads to much confusion in the literature (see Appendix A).

The above finding implies that the motion of a charged particle in a uniform magnetic field and an infinitely wide transverse wave packet may depend sensitively on the initial location of its cyclotron center with respect to the electric wave packet troughs. For most values of the x_c coordinate of the cyclotron center the width of

the instability zone decays as $\exp(-\pi^2/2K\cos x_c)$. If the x_c coordinate of the cyclotron center is near $\pi/2$ (located near an inflection point of the wave-packet envelope) then the width of the instability zone decays as $\exp(-\pi^2/K^2)$. If x_c is located on the symmetry line ($x_c = 0$), then the width of the instability zone decays as $\exp(-\pi^2/K)$. The width of the stochastic layer influences the observable dynamics. First, the probability to belong to the stochastic zone is proportional to the stochastic zone width. Second, the width of the stochastic zone determines the diffusion rate.

In the case of oblique propagation of the wave packet additional degree of freedom arises which corresponds to the motion parallel to the magnetic field. Evolution of the corresponding coordinates has substantial influence on the dynamics in the (u, v) plane. Some aspects of this dynamics in the full 4-dimensional phase space were investigated in Ref. [29]. In Ref. [21], we study some of the implications of the current work on the phase space structure of the full $2\frac{1}{2}$ d.o.f. system.

Acknowledgement

Appendix A

In this Appendix we present results for the width of stochastic layer obtained using the linearized M_4^4 map and then we point out why they are wrong for the case $x_c = 0$. This problem lead to the appearance of different results for the stochastic layer width in the literature [17,30,15]. Consider the forth iterate of the map, expand it as a power series in K and keep only first order terms. Then

$$\bar{u} = u + 2K\sin(v - x_c), \qquad \bar{v} = v - 2K\sin(\bar{u} - x_c).$$

This map corresponds to the following Hamiltonian,

$$\tilde{H} = -(K/2)\cos x_c\left(\cos v + \cos u \sum_{n=-\infty}^{\infty} \delta(\tfrac{1}{4}t - n)\right).$$

It can be represented as a sum of unperturbed integrable Hamiltonian and time-dependent perturbation,

$$\tilde{H} = H + V, \qquad H = -(K/2)\cos x_c(\cos v + \cos u) = -\Omega(\cos v + \cos u),$$

$$V = -(K/2)\cos x_c \cos u \, 2\sum_{n=1}^{\infty}\cos(n\pi t/2) = -2\Omega\cos u\sum_{n=1}^{\infty}\cos(n\pi t/2),$$

where $\Omega = \frac{1}{2}K\cos x_c$. Note, that in the first order approximation both H and V vanish for $x_c = \pi/2$.

With the assumptions on higher harmonics and separatrix form made above the separatrix map has the following form,

$$H_{n+1} = H_n + 2\pi^2\cos(\pi t_n/2)\exp(-\pi^2/4\Omega), \qquad t_{n+1} = t_n + \frac{1}{\Omega}\ln\left(\frac{8\Omega}{|H_{n+1}|}\right).$$

Then the width of the stochastic layer is given by

$$H_s = \frac{\pi^3}{\Omega}\exp(-\pi^2/4\Omega) = \frac{2\pi^3}{K\cos x_c}\exp(-\pi^2/2K\cos x_c).$$

This expression supplies the correct exponential behavior for $x_c \neq 0$ (see e.g. (27)). However, for $x_c = 0$ it gives wrong result – the coefficient in the exponent has an extra multiplier $1/2$, while the correct result is proportional to the nonleading term in (27). A possible explanation for this is that while the original map is nongeneric at $x_c = 0$, in the sense that the leading order term in the expansion for the separatrix splitting has a zero coefficient, its linearization produces a generic near-identity map for which this term has a nonzero coefficient.

References

[1] V.V. Afanasiev, A.A. Chernikov, R.Z. Sagdeev and G.M. Zaslavsky, Phys. Lett. A 144 (1990) 229.

[2] C. Amick, S.C.E. Ching, L.P. Kadanoff and V. Rom-Kedar, J. Nonlinear Sci. (1992) 9.

[3] V.I. Arnold, Dokl. Akad. Nauk SSSR 156, 9 (1964).

[4] V.I. Arnold, Dynamical systems, Vol. III (Springer Berlin, 1988).

[5] B.V. Chirikov, Phys. Rep. 52 5 (1979) 265.

[6] I. Dana and M. Amit, Phys. Rev. E 51 (1995) R2731.

[7] I. Dana, Phys. Rev. Lett. 73 (1994) 1609.

[8] D. J.D. Earn and S. Tremaine, Physica D 56 (1992) 1.

[9] E. Fontich and C. Simó, Ergod. Th. Dynam. Sys. 10 (1990) 295.

[10] V.G. Gelfreich, V.F. Lazutkin and M.B. Tabanov, Chaos 1 (1991) 137.

[11] M. Golubitsky, I. Stewart and J. Marsden, Physica D 24 (1987) 391.

[12] C. Grebogi, S. M. Hammel, J. A. Yorke and Tim Sauer, Phys. Rev. Lett. 65 (1990) 1527.

[13] S. M. Hammel, J. A. Yorke and C. Grebogi, Bull. Am. Math. Soc. 19 (1988) 465.

[14] A.N. Kolmogorov, Dokl. Akad. Nauk SSSR 119, 861 (1958); 124, 754 (1959).

[15] V.F. Lazutkin, I.G. Schachmannski and M.B. Tabanov, Physica D 40 (1989) 235.

[16] A. Lichtenberg and M. Lieberman, Regular and stochastic motion (Springer, Berlin, 1983).

[17] A. J. Lichtenberg and B. P. Wood, Phys. Rev. A 39 (1989) 2153.

[18] J.H. Lowenstein, Chaos 2 (1992) 413.

[19] J.D. Meiss, Average exit time for volume preserving maps, to appear in Chaos.

[20] V.K. Melnikov, Dokl. Akad. Nauk SSSR 148 (1963) 1257.

[21] S. Pekarsky and V. Rom-Kedar, Degeneracies and instabilities of the motion of a charged particle – the 4D web-map model , submitted preprint;
S. Pekarsky, Uniform stochastic web in Hamiltonian systems, submitted M.Sc. thesis, Weizmann institute (1996).

[22] F. Rannou, Astron. Astrophys. 31 (1974) 289.

[23] V.Rom-Kedar and S.Wiggins, Arch. Rat. Mech. Anal. 109 (1990) 239.

[24] V. Rom-Kedar, Nonlinearity 7 (1994) 441.

[25] R.Z. Sagdeev and G.M. Zaslavsky, Regular and chaotic dynamics in a magnetic field, in: Nonlinear phenomena in plasma physics and hydrodynamics, ed. R.Z. Sagdeev (Mir, Moscow, 1986).

[26] A. Tovbis, M. Tsuchiya and C. Jaffé, Chaos – integrability transition, exponential asymptotics and the saddle-center bifurcation of the Hénon map, preprint.

[27] G.M. Zaslavsky and N.N. Filonenko, Zh. Eksp. Teor. Fiz. 54 (1968) 1590.

[28] G.M. Zaslavsky, M.Yu. Zakharov, R.Z. Sagdeev, D.A.Usikov and A.A. Chernikov, Zh. Eksp. Teor. Fiz. 91 (1986) 500.

[29] G.M. Zaslavsky, M.Yu. Zakharov, A.I. Neishtadt, R.Z. Sagdeev, D.A. Usikov and A.A. Chernikov, Zh. Eksp. Teor. Fiz. 96 (1989) 1563.

[30] G.M.Zaslavsky, R.Z.Sagdeev, D.A.Usikov, A.A.Chernikov, Weak chaos and quasi-regular patterns (Cambridge Univ. Press, Cambridge, 1991).